The impact of new signals on precise marine navigation - initial results from an experiment in Harwich harbour

Alex Parkins, University College London
Alan Grant, The General Lighthouse Authorities of the United Kingdom and Ireland
Paul Cross, University College London

Alex Parkins is a PhD student in the Department of Civil, Environmental and Geomatic Engineering at University College London (UCL). He received an MSc in Surveying from UCL in 2005 and a BSc in Mathematics from the University of Warwick in 2003. He is currently studying precise GNSS positioning in the marine environment.

Alan Grant is a Principal Engineer for the Research and Radionavigation directorate of the General Lighthouse Authorities of the UK and Ireland, where he leads GNSS related projects within the directorate. He received the degrees of BSc and PhD from Staffordshire University and the University of Wales respectively. He is an Associate Fellow of the Royal Institute of Navigation, a member of the US Institute of Navigation and is a Chartered Physicist.

Paul Cross is Professor of Geomatic Engineering at UCL, a post he has held for the last twelve years. He obtained his PhD from the University of Nottingham in 1970 and before joining UCL held teaching and research positions at the Universities of Nairobi, East London, Stuttgart and Newcastle. His main research interest is in precise GNSS positioning and he currently concentrates on engineering and geophysical applications.

Abstract

The General Lighthouse Authorities of the United Kingdom and Ireland (GLAs) are supporting a project at University College London (UCL) to study whether it is possible to meet the International Maritime Organisation's (IMO) future requirements for port and harbour approach using future GNSS constellations, as detailed in IMO resolution A.915. This paper presents the results of a trial focusing on the accuracy, integrity, availability and continuity of port navigation, port approach, and docking.

The required accuracy for docking is $0{\cdot}1$ m (95%), which currently necessitates the use of Real Time Kinematic (RTK) processing. We consider the single-epoch geometry-based approach, which is robust against loss of lock and will fully benefit from the additional satellites. The trial was held at the beginning of May 2008 and saw *THV Alert* navigate into Harwich port while satellite observation data were recorded from the vessel and from shore-based reference stations. Additional data were obtained from nearby Ordnance Survey reference stations, and two total stations were used to track the vessel's passage to provide a truth model. Several modernised GPS satellites were tracked. The data were processed under different scenarios, using software developed at UCL, and the positioning performance analysed.

Providing integrity for single-epoch RTK is particularly difficult. The identification of phase observation outliers is not possible before the integer ambiguities are resolved, but an undetected outlier could prevent successful ambiguity resolution. However, it will not always be necessary to fix every ambiguity to achieve the required precision, particularly with a multi-GNSS constellation. This paper introduces a new algorithm for partial ambiguity resolution in the presence of measurement bias that has been developed and tested at UCL. This algorithm results in an improved ambiguity resolution success rate at the expense of computation time.

Keywords: GNSS; marine requirements; partial ambiguity resolution.

1 Introduction

World economic output increased by 4% in 2006 and further growth is predicted over the next few years (UNCTAD, 2007). This expansion has been driven by the performance of China and India, whose economies grew by $10{\cdot}7\%$ and $9{\cdot}2\%$, respectively, in 2006. Over 90% of global trade is carried by sea (IMO, 2005) so there have been corresponding increases in commercial maritime activity and merchant fleet capacity. Ports and seaways are busier than ever and will become more crowded in the future. Economies of scale result in ever larger and

Table 1: IMO requirements for a future GNSS (IMO, 2001)

	Accuracy	Integrity			Availability	Continuity
	Horizontal (m)	Alert limit (m)	Time to alarm (s)	Integrity risk (per 3 hours)	% per 3 days	% over 3 hours
Ocean and coastal	10	25	10	10^{-5}	99·8	N/A
Port approach	10	25	10	10^{-5}	99·8	99·97
Port navigation	1	2·5	10	10^{-5}	99·8	99·97
Automatic docking	0·1	0·25	10	10^{-5}	99·8	99·97

faster ships being built, further increasing the burden on shore infrastructure.

The International Maritme Organisation (IMO), supported by the International Association of Marine Aids to Navigation and Lighthouse Authorities (IALA), is developing an "e-navigation" strategy to promote, coordinate, regulate and standardise the use of modern technologies for the improvement of navigational safety:

> "e-navigation is the harmonised collection, integration, exchange, presentation and analysis of maritime information onboard and ashore by electronic means to enhance berth to berth navigation and related services, for safety and security at sea and protection of the marine environment." (IMO, 2008)

Many of the technologies required for this are already available and in use. Automatic Identification Systems (AIS) transmit positional information to other ships and to shore stations; Electronic Chart Display and Information Systems (ECDIS) allow this information to be displayed on up-to-date electronic charts; and Vessel Traffic Services (VTS) allow port and harbour authorities to monitor vessel movements. IALA (2008) provides more information about the need for e-navigation and its development.

E-navigation can be expected to bring about substantial benefits to marine safety and efficiency. However, it is dependent on a precise and robust positioning system. Although back-up systems such as eLoran might be used, the primary positioning system will be GNSS (de Halpert et al, 2006).

The United States is currently in the process of modernising GPS, increasing the number of available civil signals. The first modernised signal available is a civil code on L2, currently transmitted by six Block IIR-M satellites. Next will come a new signal, L5, which will be transmitted by a Block IIR-M and Block IIF satellites in 2009. By 2013 the final stage in GPS modernisation may have begun: Block III satellites which will feature an improved code on L1 and increased transmission power.

The Galileo system of 30 satellites will provide freely accessible civil signals overlaid on, and with very similar characteristics to, the GPS L1 and L5 frequencies, called E1 and E5a. There will be an additional civil signal, E5b, adjacent to E5a, and a commercial encrypted signal, L6. Galileo is designed to be compatible and interoperable with GPS, so a receiver can easily track both constellations at L1 and L5.

The IMO recognises the importance of GNSS to the future of marine navigation and has established requirements for a future GNSS (IMO, 2001). As well as operational and institutional requirements, there is a comprehensive set of requirements on the performance of a future GNSS. Requirements are set out for a number of applications: Table 1 shows a few of the most general.

To enable an analysis of how the requirements may be met, GPS data were collected from onboard a ship entering Harwich harbour and coming to dock, whilst being tracked by two total stations as a truth model. Software was developed to enable the data collected to be processed using a variety of different techniques and models.

This paper describes the process of collecting and analysing the data. Section 2 describes the data collection exercise and the process of generating the truth model. Section 3 describes the techniques used to process the data, as well as a novel algorithm to enable a subset of ambiguities to be resolved in the presence of measurement bias. Section 4 gives the results of the data processing, analysed with respect to the IMO requirements of Table 1.

2 Data collection

2.1 Data collection

The data collection exercise was carried out in Harwich on the evening of 1st June 2008, onboard the ship *THV Alert*. Three Topcon GR-3 GPS receivers, capable of tracking the modernised signal on L2, were used: the rover mounted on the stern of *THV Alert* (SHIP); a reference station on the roof of the nearby Trinity House building (BASE); and a second reference station in an open field 10 km away (WIX). Additional data were obtained from nearby Ordnance Survey reference stations, as shown in Figure 1. All GPS receivers were operated at a data rate of at least 1 Hz. A prism was mounted underneath the antenna

on *THV Alert* and tracked by total stations from the shore, as shown in Figures 2 and 3. This provided a truth model for the GPS data.

Figure 4 shows the area of the data collection exercise. Topcon GPT-9000A automatic tracking total stations were set up at JETTY and NAVY. The pink track shows the course of *THV Alert* as she made several approaches to the jetty, simulating port approach and docking. As the ship turned, the rover was transferred to the side closest to the shore to maximise the prism visibility.

2.2 Generation of truth model

2.2.1 Technique

A total station measures the angle and distance to the prism at a non-constant rate of ~ 3 Hz: these observations were used to provide a truth model for the GPS positions, which were projected to a plane using a Transverse Mercator projection, and transformed to the local coordinate system. The positions obtained when the ship was turning and the rover was moved to the other side of the ship were excluded. The raw prism positions (green and red positions in Figure 5) are much less smooth than expected from the motion of the ship. Analysis of the observations showed that the total station did not always update the range or angle observations before output: of the 38,427 sets of observations from both total stations, 78% had updated range and 44% updated horizontal angle; both range and angle were updated in 24% of epochs, and neither were updated in 2% of epochs. Vertical angle was not considered due to the slow rate of change. The range is measured to the nearest centimetre, and the angle to 5" (≈ 1 cm at 400 m); the target was moving at 1 m/s, so it is unlikely that the true observation was constant to this precision for any significant period of time. The raw prism positions therefore do not represent the true path of the ship, because of the substantial error introduced in the measurement update process. Those positions with both observations updated (red), show less noise but are too sparse to allow comparison to the 1 Hz GPS data.

In order to obtain a smooth track with enough positions for comparison with GPS, the un-updated measurements were estimated by linear interpolation between the nearest updated measurements: most positions are therefore determined from a combination of interpolated and observed parameters. Figure 5 shows that these positions (blue) exhibit much less noise than the raw positions. The subsequent analysis is performed on the union of the positions with both observations updated (red) and positions with at least one interpolated observation (blue).

The total stations did not measure at the same instant as the GPS receiver, so each set of total station positions were linearly interpolated in time to match

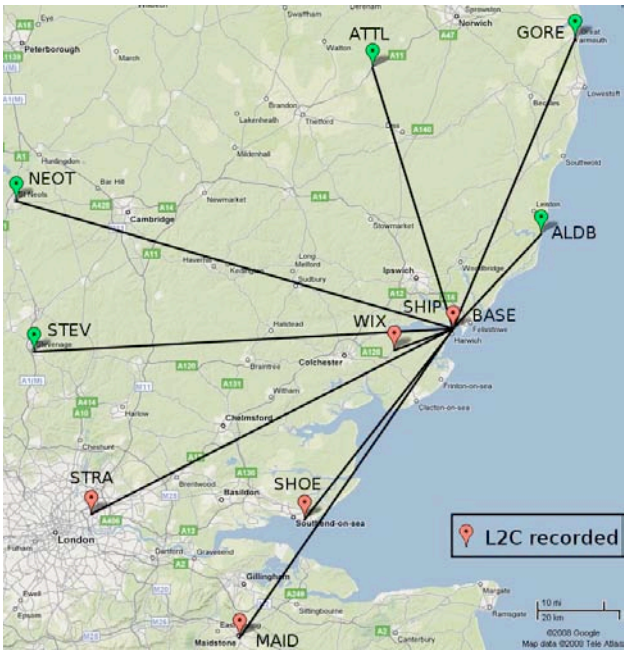

Figure 1: Map of reference stations

Figure 2: Total station tracking *THV Alert*

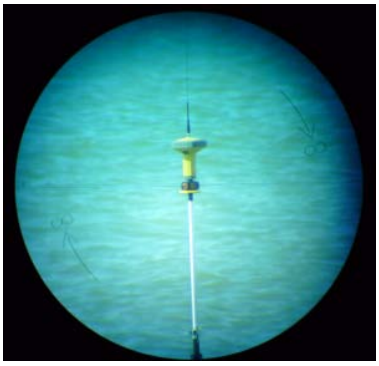

Figure 3: GPS receiver and prism on *THV Alert*, viewed through the total station telescope

Figure 4: Plot of *THV Alert*'s course, showing total station locations with 400 m range circles

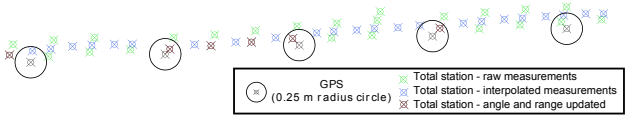

Figure 5: GPS and prism positions

the GPS epoch. If the GPS position at epoch l is

$$P(l)_{\mathsf{GPS}} = \left(E(l)_{\mathsf{GPS}}, N(l)_{\mathsf{GPS}}\right) \tag{1}$$

then the interpolated prism position to match the GPS position is:

$$\begin{aligned} P(l)_{\mathsf{TS}} = (&E(k)_{\mathsf{TS}} + a\left(E(m)_{\mathsf{TS}} - E(k)_{\mathsf{TS}}\right), \\ &N(k)_{\mathsf{TS}} + a\left(N(m)_{\mathsf{TS}} - N(k)_{\mathsf{TS}}\right)), \end{aligned} \tag{2}$$

where

$$P(k)_{\mathsf{TS}} = \left(E(k)_{\mathsf{TS}}, N(k)_{\mathsf{TS}}\right) \tag{3}$$

is the nearest prism position in the past;

$$P(m)_{\mathsf{TS}} = \left(E(m)_{\mathsf{TS}}, N(m)_{\mathsf{TS}}\right) \tag{4}$$

is the nearest prism position in the future; and

$$a = \left(t(l) - t(k)\right) / \left(t(m) - t(k)\right). \tag{5}$$

The total station time-stamps are based on a local clock rather than GPS time, so a least-squares adjustment was performed to solve for the difference between the time systems. This was modelled as a constant offset δt and linear drift Δt of each local clock from GPS time:

$$t(i)_{\mathsf{GPS}} = t(i)_{\mathsf{TS}} + \delta t + \left(t(i)_{\mathsf{TS}} - t(1)_{\mathsf{TS}}\right)\Delta t, \tag{6}$$

where $t(i)$ is the time of the current epoch and $t(1)$ is the time of the first epoch. δt was kept small by synchronising the local clocks to GPS time at the start of the exercise. For each epoch l the ship's velocity was estimated from the interpolated prism positions:

$$\begin{aligned} V(l) &= \left(V_E(l), V_N(l)\right) \\ &= \left(\frac{E(l+1) - E(l)}{t(l+1) - t(l)}, \frac{N(l+1) - N(l)}{t(l+1) - t(l)}\right) \end{aligned} \tag{7}$$

The least-squares adjustment is set up as follows:

$$A = \begin{bmatrix} V_E(1) & V_E(1)\left(t(1) - t(1)\right) \\ V_N(1) & V_N(1)\left(t(1) - t(1)\right) \\ \vdots & \vdots \\ V_E(M) & V_E(M)\left(t(M) - t(1)\right) \\ V_N(M) & V_N(M)\left(t(M) - t(1)\right) \end{bmatrix} \tag{8}$$

$$x = \begin{bmatrix} \delta t \\ \Delta t \end{bmatrix};\ b = \begin{bmatrix} P^E_{\mathsf{GPS}}(1) - P^E_{\mathsf{TS}}(1) \\ P^N_{\mathsf{GPS}}(1) - P^N_{\mathsf{TS}}(1) \\ \vdots \\ P^E_{\mathsf{GPS}}(M) - P^E_{\mathsf{TS}}(M) \\ P^N_{\mathsf{GPS}}(M) - P^N_{\mathsf{TS}}(M) \end{bmatrix} \tag{9}$$

where M is the number of epochs with an interpolated prism position corresponding to a GPS position. The parameters are the solved as:

$$x = A^{-1}b \tag{10}$$

Equation 2 and Equation 10 were solved iteratively until convergence. Table 2 gives the computed clock offset and drift: it appears that the local clock at JETTY was not correctly synchronised to GPS time. Over the period of the data collection exercise, the clock at NAVY advanced by $0{\cdot}04$ s and the clock at JETTY advanced by $0{\cdot}08$ s. The ship is moving at

Table 2: Offset and drift of total station clocks from GPS time

Station	Clock offset (s)	Clock drift
NAVY	$-1{\cdot}04$	$8{\cdot}5 \times 10^{-6}$
JETTY	$-14{\cdot}94$	$1{\cdot}8 \times 10^{-5}$

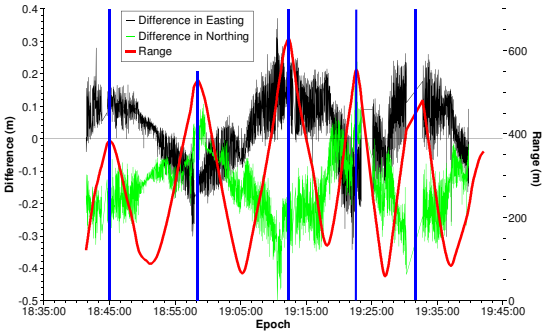

(a) NAVY

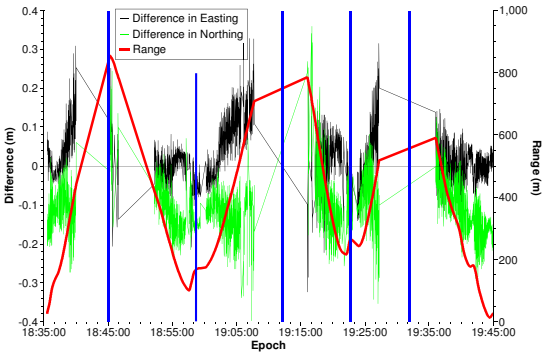

(b) JETTY

Figure 6: Difference between GPS and prism positions

> 1 m/s so, if not solved for, the clock drift would bias the final result by several centimetres.

The result of these adjustments is a set of prism positions from each total station with the same time-stamps as the GPS positions, in GPS time. These can then be directly compared to the GPS positions.

2.2.2 Results

Figure 6 shows the plan difference between the GPS and prism positions for each station, with the different "runs" (periods between turns) delimited by vertical blue lines. The gaps in the data are periods when the total station could not see the prism: there was worse visibility from JETTY than from NAVY. There was an unexpected offset between the GPS and prism positions, which is not constant but follows a distinct pattern that repeats with each run. There is an average

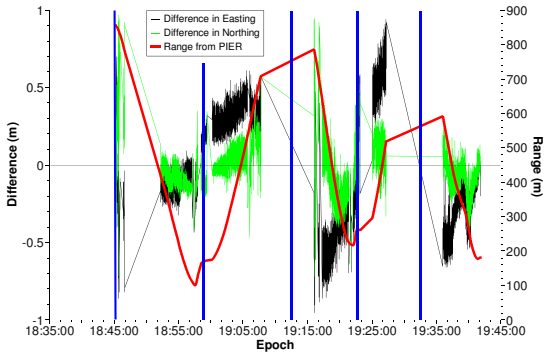

Figure 7: Difference between prism positions from NAVY and JETTY

offset in Northing of $14{\cdot}1$ cm from NAVY and $10{\cdot}1$ cm from JETTY; Easting offsets are much smaller at $0{\cdot}7$ cm and $-2{\cdot}4$ cm respectively. The ship's movement is mainly in the East-West direction, so some of the error in this direction may have been absorbed by the calculation of the clock offset in Equation 10.

Figure 7 shows the plan difference between prism positions after the iterative interpolation and time offset adjustments were applied to the two sets of prism positions (the positions from JETTY were adjusted to match the time-stamps and clock time of the positions from NAVY). The correspondence is worse between the two total stations ($\sim 0{\cdot}5$ m) than between either total station and GPS ($\sim 0{\cdot}2$ m). This implies that the poor agreement with GPS is substantially due to low total station measurement precision.

As discussed in Section 2.2.1, the total stations output positions at a rate of around 3 Hz, but the observations are not necessarily updated from the previous position. This implies that data output is not dependent upon obtaining an updated measurement. Therefore even when both measurements have been updated, the range and angle measurements are not necessarily synchronous, and the time-stamp records when the measurements were output rather than when they were obtained. These factors introduce significant error to the prism positions for a moving target. The interpolation and clock adjustment process will also introduce error, particularly during the periods when the ship is turning; interpolation errors should be smaller on the straight sections. The strictest IMO requirement on accuracy (95%) for a future GNSS is $0{\cdot}100$ m and the agreement between the total stations is $0{\cdot}283$ m: the total station measurements are not sufficiently precise to provide a truth model for these requirements.

2.2.3 Ambiguity validation

If the GPS ambiguities have been resolved correctly then the maximum error on any single GPS observation is $1/2$ cycle (10 cm for L1 and 12 cm for L2): this

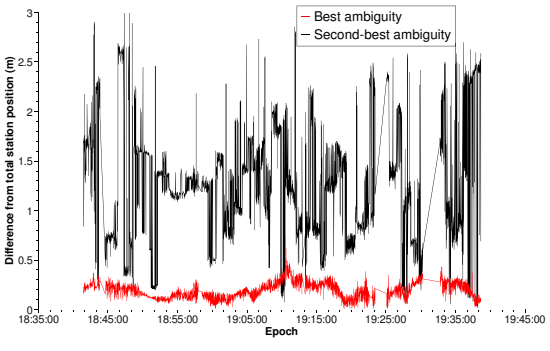

(a) NAVY

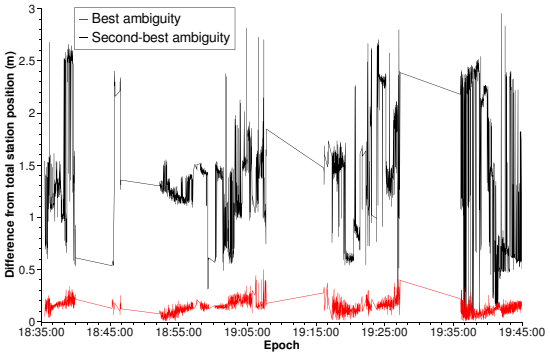

(b) JETTY

Figure 8: Difference between prism and GPS positions with best and second-best ambiguities

is therefore also the maximum position error. Over the very short baseline from BASE to SHIP (< 1 km), spatially correlated errors will almost completely cancel and the dominant error source will be phase multipath with a maximum magnitude of $1/4$ cycle (6 cm for L2). Therefore, assuming the ambiguities have been correctly resolved, the GPS positions should be more accurate than the prism positions.

The total station measurements can be used to validate the short-baseline ambiguity resolution. As discussed in Section 3, the LAMBDA method for ambiguity resolution selects the set of integers that minimise the sum of the squares of the distances to the (real valued) float ambiguities in the metric of the float ambiguity covariance matrix. If the sets of integers are ordered by increasing sum of the squares of the distances from the float values, then the first set is the most likely (in the least-squares sense) to be the correct set. If the first set is incorrect, the second set is subsequently the most likely to be correct. Therefore a study of how close the GPS positions generated by the first and second ambiguity sets are to the prism positions can be used to validate the ambiguity resolution.

Figure 8 shows the difference between the prism positions and the GPS positions with the first and second sets of ambiguities from each total station. In general, the first ambiguity position is closer to the prism position than the second. However, there are some epochs where the second ambiguity positions are the closest: this is particularly obvious around 19:10 from NAVY.

In the processed data, the first set of ambiguities only changes after a satellite has been lost and reacquired, or when the reference satellite changes: this is in contrast to the second set, which often changes rapidly. For example, during the span $19{:}09{:}51$ - $19{:}10{:}27$, where there are 23 points where the second ambiguity positions are closest to the NAVY prism positions, the second ambiguity set varies between 3 different values but the first ambiguity set stays the same. This suggests that the first ambiguity set is indeed correct, and the difference from the prism positions is due to error in the total station measurement.

The second ambiguity position is closest in fewer than 1% of epochs, and the first set of ambiguities remains constant throughout the data collection exercise, apart from reference satellite changes and reacquisitions. Therefore, although not in themselves sufficiently accurate to provide a truth model, the total station measurements provide confidence in the short-baseline ambiguity resolution, and these GPS positions are used as the truth in subsequent analyses.

2.3 Analysis of code multipath

Analysis of the quality of the measurements at the receivers can help interpret the results. The MP_1 observable is used to estimate the magnitude of code multipath on L1:

$$\mathrm{MP}_1 = P_1 - 4{\cdot}0915\phi_1 + 3{\cdot}0915\phi_2 \qquad (11)$$

where P_1 and ϕ_1 are the code and phase observations on L1, and ϕ_2 the phase observation on L2. The noise level of this value gives an indication of code noise and multipath error. Figure 9 shows MP_1 plotted for the three GR-3 receivers, and the Ordnance Survey receiver at Aldeburgh (ALDB). The values have been centred on zero and jumps associated with cycle slips removed.

The MP_1 observable from BASE is very noisy, indicating high levels of multipath: the receiver was located on the roof of the Trinity House building and substantial multipath would have been caused by nearby surfaces. In contrast, WIX, in an open field with a clear view of the sky, shows less multipath. SHIP shows relatively better performance than expected, given the location below the ship's superstructure. The MP_1 observable at ALDB is representative of the Ordnance Survey stations: the code measurements are phase-smoothed, so there is very

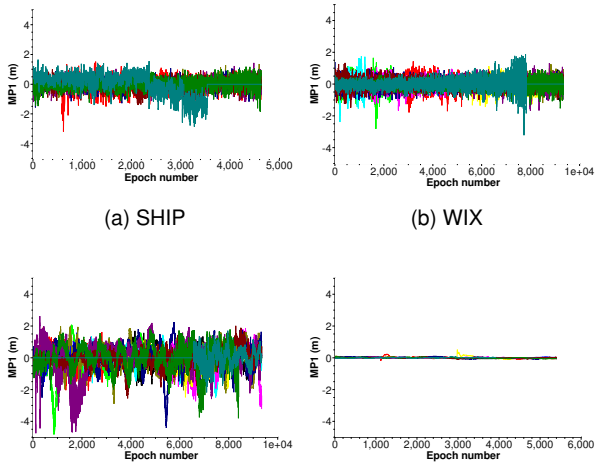

(a) SHIP (b) WIX

(c) BASE (d) ALDB

Figure 9: MP1 observables

little observable code noise and multipath (phase-smoothing was disabled for the GR-3 receivers).

3 Data processing techniques

This section describes the techniques used to process the data. There are three techniques used: point positioning (PP), which is the least precise but does not rely on shore infrastructure; differential GPS (DGPS), which uses a shore-based reference station to reduce errors over a wide area; and real-time kinematic (RTK), which uses the phase data to achieve high precision, but requires a nearby reference station and a good quality receiver.

3.1 PP

Point positioning uses the code observations to produce a positioning solution. At a receiver r, for each satellite s and for each frequency, the observation equation at time t is:

$$P_r^s(t) = \rho_r^s(t) + c\left(dt_r(t) - dt^s\left(t - \pi_r^s\right)\right) + \epsilon_r^s(t) \quad (12)$$

where:

$P_r^s(t)$	is the code observation
$\rho_r^s(t)$	is the geometric range
$dt_r(t)$	is the receiver clock offset at reception time
$dt^s\left(t - \tau_r^s\right)$	is the satellite clock offset at transit time
$\epsilon_r^s(t)$	is the remaining error

$\epsilon_r^s(t)$ encompasses many error sources that are not solved for, such as atmospheric error, orbit error, multipath and code noise. The ionosphere is a major source of error, and can be cancelled in a multi-frequency system by forming the ionosphere-free observable:

$$P_{r,IF}^s := \frac{f_1^2}{f_1^2 - f_2^2} P_{r,f1}^s - \frac{f_2^2}{f_1^2 - f_2^2} P_{r,f2}^s \quad (13)$$

where $P_{r,i}^s$ and f_i are the observation and frequency, respectively, of observable i. Ionospheric error is cancelled, but code noise and multipath is increased. Phase-smoothing is often used to reduce these error sources: the precise difference in receiver-satellite range between epochs derived from the phase observations is used to reduce the noise of the code measurements.

3.2 DGPS

The next most precise positioning technique differences the code measurements with those from a reference station to reduce errors. This is equivalent to estimating the error at a known point and then removing this error from the rover observations. For a receiver r_1, reference station r_2, satellite s, the single-differenced observation equation at time t is:

$$\begin{aligned} P_{r_1,r_2}^s(t) &= P_{r_2}^s(t) - P_{r_1}^s(t) \quad (14) \\ &= \rho_{r_1,r_2}^s(t) + c\left(dt_{r_2}(t) - dt_{r_1}(t)\right) + \epsilon_{r_1,r_2}^s(t) \end{aligned}$$

The satellite clock error cancels completely; ionosphere, troposphere and satellite orbit errors are spatially correlated and are reduced proportionally to the baseline length.

3.3 RTK

The most precise technique uses the phase observations as precise ranges. The measured observations are usually double-differenced: the single differences from each satellite are subtracted from the reference (highest elevation) satellite. The phase observations are biased by an unknown number of whole cycles between the receiver and the satellite. For a receiver r_1, reference station r_2, satellite s_1 and reference satellite s_2, the double-differenced observation equation at time t is:

$$\Phi_{r_1,r_2}^{s_1,s_2}(t) = \rho_{r_1,r_2}^{s_1,s_2}(t) + \lambda a_{r_1,r_2}^{s_1,s_2} + \epsilon_{r_1,r_2}^{s_1,s_2}(t) \quad (15)$$

where $\Phi_{r_1,r_2}^{s_1,s_2}(t)$ is the double-differenced phase observation, $a_{r_1,r_2}^{s_1,s_2}$ the integer ambiguity and λ the wavelength. Precise RTK positioning relies on the estimation of the integer ambiguities in order to use the phase observations as precise ranges. This is usually done in a four step procedure, as shown in Figure 10. The ambiguities are estimated as real-valued numbers in the float solution. The ambiguity resolution step determines the most likely set of integer values and the validation step determines if there is sufficient confidence in the best set of integers to use them (using the incorrect set can result in a position error of

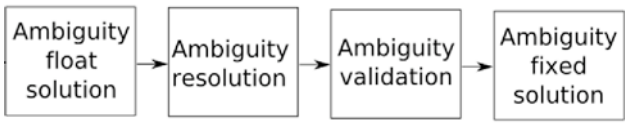

Figure 10: RTK positioning procedure

several metres). If the validation test is passed then the ambiguity-fixed solution is performed, using the phase measurements to achieve a high-precision solution.

3.3.1 Ambiguity-float solution

There are two choices to be made concerning the float solution. The first is between the geometry-based and geometry-free model. In the geometry-based model, the baseline between the rover and the reference station is parameterised in terms of the unknown rover co-ordinates; in the geometry-free model, a parameter is introduced for each double-differenced satellite-receiver range. Although the geometry-free model is simpler, the geometry-based model takes advantage of the satellite geometry and requires the estimation of fewer parameters, so it generally provides a stronger solution. The geometry-based model is used for this processing.

A single-epoch phase measurement does not contain any range information, because of the unknown real-valued ambiguity parameter. Therefore, when using this least-squares technique, it is not possible to estimate the ambiguities or derive a position in a single epoch using phase data alone. There are two solutions to this problem: either phase data are collected over multiple epochs, so that the changing satellite positions provide the range information, or the single-epoch phase data is combined with with code observations. The latter technique is used in this analysis. Although the single-epoch approach may result in fewer epochs with fixed ambiguities, it has the advantage that, in the event of loss of satellite lock, re-acquisition of the ambiguities is instantaneous, which is a significant benefit in harsh environments. Undetected cycle slips and slowly growing errors also do not pose a problem. The single-epoch solution is therefore a more robust positioning technique, which is also easier to analyse from the perspective of meeting the IMO requirements.

3.3.2 Ambiguity resolution

There are many different techniques for ambiguity resolution: Kim and Langley (2000) give a good overview. Here the LAMBDA integer least squares technique is used (Teunissen, 1993, 1995; de Jonge and Tiberius, 1996). This produces the optimal solution in the sense that it maximises the success rate. The set of integers chosen, $\breve{a}$, is the one that minimises the sum of the squares of the distances to the float values, $\hat{a}$, in the metric of the float ambiguity covariance matrix, Q_a, i.e.

$$\breve{a} = \arg\min_{z \in \mathbb{Z}^n} \|\hat{a} - z\|^2_{Q_a} \tag{16}$$

3.3.3 Ambiguity validation

After the most likely set of ambiguities is found, it is necessary to apply a further test to determine if there is sufficient confidence to use these values. There are many techniques that may be used for ambiguity validation: see Verhagen (2005) for an overview. The validation test used in this analysis is the commonly used ratio test. The integer set $\breve{a}$ is accepted if

$$\frac{\|\hat{a} - \breve{a}'\|^2_{Q_a}}{\|\hat{a} - \breve{a}\|^2_{Q_a}} > k \tag{17}$$

where $\breve{a}'$ is the second-best set of integers and k is the critical value. There is no sound theoretical basis for the choice of k; for this analysis $k = 2{\cdot}5$, a commonly used value.

3.3.4 Ambiguity-fixed solution

Once the ambiguities have been fixed and the validation test passed then the fixed solution is performed. The double-differenced phase observations with known ambiguity values are used as precise ranges to determine the final coordinates.

3.4 Partial ambiguity resolution

It is often not necessary to fix all ambiguities to obtain the required ambiguity-fixed precision, and in some circumstances fixing a subset of the ambiguities may improve the success rate. Teunissen (1999) uses the easy-to-compute integer bootstrapping success rate as a lower bound for the LAMBDA success rate:

$$P\left(\hat{a} = \bar{a}\right) \leq \prod_{i=1}^{n} \left(2\Phi\left(\frac{1}{2\sigma_{a_{i\ I}}}\right) - 1\right) \tag{18}$$

where

$$\Phi\left(x\right) = \int_{-\infty}^{x} \frac{1}{2\pi} \exp\left(-\frac{1}{2}y^2\right) dy \tag{19}$$

and $\sigma_{a_{i\ I}}$ is the conditional standard deviation of $\hat{a}_i$.

The double-differenced ambiguities are highly correlated; Equation 18 is a closer lower bound when applied to ambiguities that are almost decorrelated, which can be achieved by a linear combination generated as part of the LAMBDA algorithm. Equation 18 implies that each successive ambiguity fixed reduces the total probability of success. However, this does not necessarily mean that additional satellites

or frequencies will be detrimental to ambiguity resolution, because they may facilitate a more powerful decorrelation transformation. For the geometry-free model, where each satellite is effectively treated individually, additional satellites reduce the overall success rate because there are more ambiguities to fix, but additional frequencies increase the success rate by allowing more powerful decorrelations between the frequencies. Partial ambiguity fixing in the geometry-free model is effectively fixing a linear combination of observations from the same satellite, such as the widelane combination. For the geometry-based model, both additional frequencies and additional satellites provide a more powerful decorrelation adjustment, increasing the overall success rate. Partial ambiguity fixing still increases the success rate, but the un-fixed ambiguities are a linear combination of observations from many other satellites and frequencies.

3.5 Partial ambiguity resolution in the presence of biased observations

Biases in phase observations, such as high multipath, may cause ambiguity resolution to either fail or be incorrect. When collecting data over multiple epochs, it is possible to detect and exclude biased observations in the float solution, before ambiguity resolution takes place: the phase observations provide range information, and therefore a biased observation will have a high residual. However, when using the single-epoch approach this is not possible because each double-differenced phase observation has a corresponding real-valued ambiguity estimate: the bias in the phase observation translates directly to a bias in the ambiguity estimate. Hence the phase observation residuals are zero and it is not possible to detect a bias before ambiguity resolution is performed.

With the geometry-free model, where each satellite is effectively treated independently, incorrect ambiguity resolution only affects the ambiguities from the satellite with the biased observation. The position error will therefore be relatively small, and it is possible to detect and exclude observations with incorrect ambiguities at the ambiguity-fixed stage. However, with the geometry-based model, due to the high correlation of the ambiguities, a bias in a single observation can cause all ambiguities to be resolved incorrectly, to values far from the truth. This can cause a position error of several metres, as seen in Figure 8, and it will not be possible to detect the bias at the ambiguity-fixed stage because all observations will have incorrect ambiguities and the biased observation will not have an unusually high residual.

Therefore a problem that applies uniquely to the single-epoch geometry-based approach is that it is not possible to detect a phase observation bias before ambiguity resolution is performed, and the undetectable bias can cause ambiguity resolution to either fail, or to introduce undetectable biases into the positioning solution which may produce position errors of several metres.

When Galileo and modernised GPS are operational, a receiver will be tracking a much greater number of signals. It is therefore more likely that at least one of these phase observations will contain a bias that will affect the ambiguity resolution of the whole set of ambiguities. This effect is somewhat mitigated by the improved ambiguity resolution robustness when using the geometry-based model with the additional signals and satellites. However, it may be beneficial to develop an approach to allow a subset of the ambiguities to be fixed in the presence of measurement bias.

3.5.1 Algorithm description

An algorithm for partial ambiguity resolution in the presence of biased observations, illustrated in Figure 11, is now described. The algorithm is only applied if the ambiguity validation test fails when using the full set of ambiguities. All subsets of the full set above a certain size are generated and ordered according to some criterion. The normal ambiguity resolution and validation procedure is then applied to each subset in turn: the first subset that passes the ambiguity validation test is accepted. It is therefore highly likely that a set of fixed ambiguities will be obtained, and by trying the "best" subsets first it is more likely to be correct. The subsets can be ordered according to many criteria:

- Ratio: Increasing distance of integers from the float values (this has the disadvantage that all subsets must have LAMBDA run on them);
- Decreasing ambiguity precision (determinant of the covariance matrix): start with the most precise observations, which are the most robust to bias;
- External information such as signal to noise ratio: start with the observations that are least likely to be be biased;
- Increasing ambiguity dilution of precision (ADOP) (see Teunissen et al (2000)). This combines precision with the number of observations;
- A combination of the above (e.g. $^{\text{mean SNR}}_{\text{ADOP}}$: start with the observations that are least likely to contain a bias and are most robust against it).

ADOP is easy to compute and gives good results, so this is used in subsequent analyses.

This algorithm is rather computationally intensive, as the ambiguity resolution algorithm is run multiple times. However, it is currently feasible for post-processing, and could be possible for a mobile re-

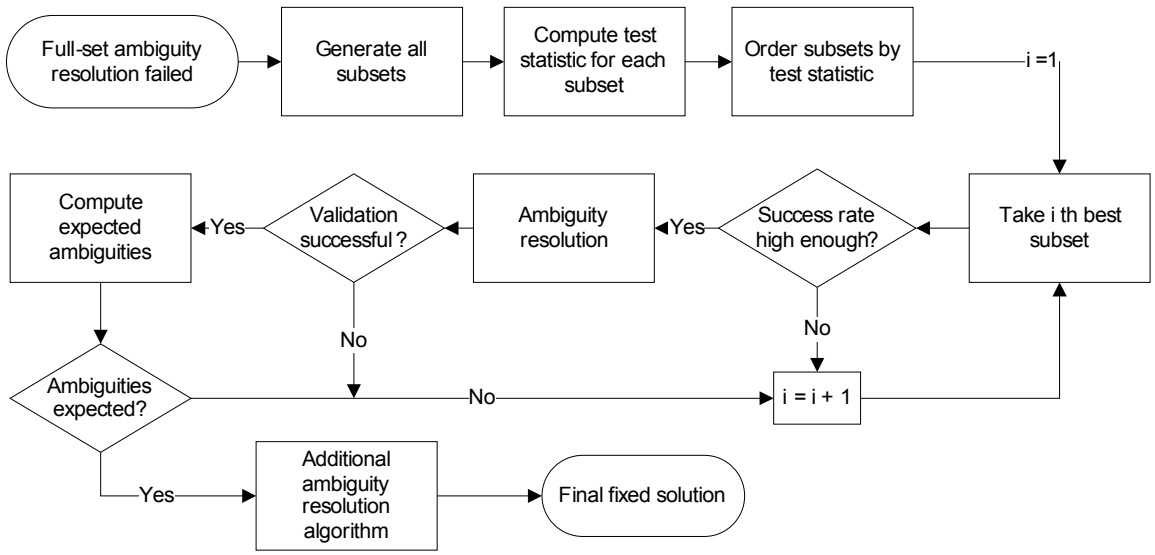

Figure 11: Subset ambiguity resolution algorithm

ceiver in the future with increased receiver processing power. It is an ideal candidate for multi-threading, since it relies on many runs of the same function. It could also be used in situations where the rover sends its observations to a base station for processing.

The algorithm is only run if normal ambiguity resolution has failed, so can only improve the success rate: tests have shown that a substantial improvement can be obtained (see results in Section 4). Every time the algorithm attempts to fix a subset, there are two types of error that can be made when applying the validation test. A Type I error, rejecting the correct ambiguities, has little effect, because there are many more such subsets to try to fix. However, a Type II error, accepting the ambiguities when they are false, is much more serious: position errors of several metres can be introduced. This is therefore much worse than if the algorithm was not run and no position was returned. Tests have shown that Type II errors can occur in a significant proportion of epochs, so the algorithm must be modified to make it viable.

3.5.2 Reducing Type II error probability

Several techniques are applied to reduce the probability of making a Type II error. If, for a given subset, the probability of successful ambiguity resolution (given by Equation 18) is below a given value then ambiguity resolution is not attempted; even if the validation test were passed, there would still be a high probability of making a Type II error with this subset. However, this technique alone is not sufficient to reduce the incidence of Type II error to an acceptable level.

The second technique is a fundamental change in concept: instead of allowing the fixed ambiguity set to take any value, it is only accepted if the values obtained are identical to those predicted from the previous epochs. Only epochs in which the entire set was fixed (i.e. not using this algorithm) are used for prediction. Therefore the algorithm can not be used to fix ambiguities independently, but can fill in gaps between epochs where a bias on one or more observations prevents successful ambiguity resolution, as long as the ambiguities do not change. The predicted values are generated by taking the weighted mode of the values for each ambiguity over a fixed number of previous epochs. The weighting decays with time, so more recent values have more influence on the predicted value. If the ambiguities change then it will take a few epochs of correct fixing before the predicted values are correct.

With this modification, the algorithm is immune to Type II error except in the case where the expected values are incorrect, and the algorithm fixes an ambiguity subset to these values. The prediction will be incorrect in two circumstances: if in several previous epochs the ambiguities have been fixed to the same incorrect values, or if the ambiguities change and the algorithm fixes a subset to the previous values. The latter seems rather unlikely; the former is more likely but would be perpetuating the error from the standard ambiguity resolution, so is not a new source of error. However, this is still a risk to be aware of.

3.5.3 Improving positional precision

A potential problem with the subset ambiguity resolution algorithm is that there may be too few observations remaining to allow a sufficiently precise final position. A further algorithm is therefore used to fix am-

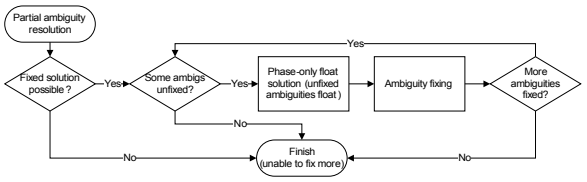

Figure 12: Additional ambiguity resolution algorithm

biguities that were not fixed during the initial subset ambiguity resolution process. A least-squares adjustment is carried out, similar to the conventional float solution in that unknown ambiguities are included as parameters, but in this case the fixed phase observations provide the range information. These are more precise than the code observations used in the original float solution, so provide a greater probability of fixing the remaining ambiguities. The subset ambiguity resolution algorithm is then applied to the remaining float ambiguities: this is an iterative process which will end when either all the ambiguities have been fixed or the subset ambiguity resolution fails to fix any more. This is illustrated in Figure 12.

4 Results

4.1 Processing technique

The data collected in Harwich harbour are processed with regards to the IMO requirements for a future GNSS outlined in Table 1. As discussed in Section 2, the short-baseline RTK positions from BASE are used as the truth model: tracking total stations were used to provide confidence that the ambiguity resolution is correct. The dominant error source over this short baseline is phase multipath, with a maximum magnitude of $1\ 4$ cycle: therefore the GPS positions should be accurate to within 6 cm.

The aim of the data analysis is to determine which processing techniques meet which sets of requirements. The IMO requirements are not specific enough to be directly applied to real data, so some assumptions are made to facilitate analysis. Accuracy is taken as the 95th percentile of the difference between the obtained positions and the truth; integrity risk is the proportion of 10 s spans containing at least one integrity error and no valid positions (causing an integrity breach); availability is the percentage of 10 s spans that contain at least one valid position; and continuity is the percentage of the total experiment time covered by the longest span with no 10 s gaps. 10 s is the time-to-alarm for the integrity requirement: the requirements allow an undetected position error for this period of time before an integrity breach is declared. It therefore seems reasonable to allow the same grace period if the receiver returns no position, which is a less dangerous outcome. If this assumption is not made then it would be very hard to meet the continuity and availability requirements, particularly with RTK. There is no specification for height performance, so only the plan positions are considered.

4.2 Point positioning

The accuracy was $3{\cdot}514$ m with L1 only, $3{\cdot}283$ m with dual frequency and $3{\cdot}285$ m with dual frequency using the ionosphere-free linear combination. The ionospere-free combination, although eliminating ionospheric noise, did not improve the accuracy: data were collected at a time of relatively low ionospheric activity, and the high multipath and code noise are multiplied. These accuracies are too low to meet the port navigation requirement of 1 m, but can easily meet the port approach requirements (10 m). The integrity, availability and continuity requirements were all met.

4.3 DGPS

The DGPS positions for all baseline lengths are not sufficiently accurate to meet the automatic docking requirements ($0{\cdot}1$ m accuracy), so they are analysed with respect to the port navigation requirements. The integrity, availability and continuity requirements were met for all baseline lengths. Figure 13 shows the accuracy with respect to the 1 m requirement: this is met for all baseline lengths for both single and dual frequency. The correlation between accuracy and baseline length is low, so it is likely that the requirements could be met over even longer baselines; the multipath error dominates the single-difference atmospheric and satellite orbit errors. However, this may not be the case in times of high ionospheric activity, and if the ionosphere-free observable were used then the increased noise would prevent the port navigation accuracy requirements from being met.

These results are produced with phase-smoothing applied. Without it, the accuracy from BASE (1 km baseline) is $1{\cdot}261$ m for dual frequency: higher than the requirement. This is due to high code multipath at the reference station, as shown in Figure 9. This shows how significant code multipath can be, and the effectiveness of phase in reducing it.

4.4 RTK

The RTK solution, with correct ambiguity resolution, is capable of meeting the strictest accuracy requirement, $0{\cdot}1$ m for automatic docking. The data are therefore processed with regard to this requirement. The subset ambiguity algorithm described in Section 3.5 is also applied to determine its effectiveness.

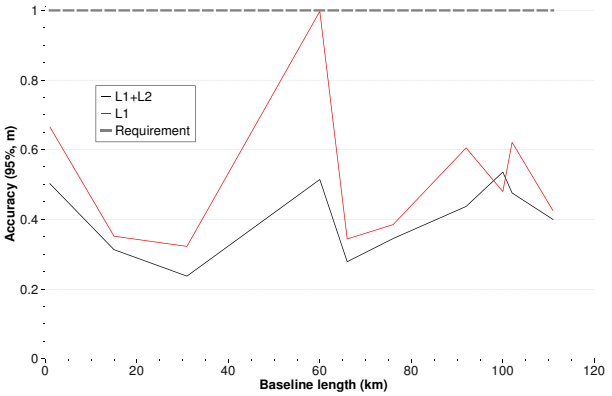

Figure 13: DGPS accuracy

Figure 14a shows the accuracy results: the poor accuracy for single frequency is caused by incorrect ambiguity resolution, which did not occur for dual frequency except over the longest baselines. The peak at 100 km for the dual-frequency subset ambiguity resolution is caused by the propagation of ambiguities that had been incorrectly resolved using LAMBDA. The short-baseline data are the truth model, and so have perfect accuracy.

Integrity errors are caused by incorrect ambiguity resolution, and begin to appear at longer baselines. However, only with single-frequency data do enough occur to cause integrity breaches, as shown in Figure 14b. Due to the small amount of data analysed, even a single integrity breach is enough to cause an integrity risk much greater than the requirements allow.

Availability and continuity are the hardest requirements for RTK to meet; they are related to the ambiguity resolution success rate, which rapidly decreases with increasing baseline length due to atmospheric and orbit error decorrelation. Figures 14c and 14d, show that it is not possible to meet the availability and continuity requirements using L1 alone. Using dual frequency, the requirements are met for the 1 km baseline, but not over any greater distance. The subset ambiguity resolution technique increases the viable baseline length to 66 km.

4.5 Analysis of L2C residuals

Several stations recorded both L2 and the new civil signal, L2C, from the three visible Block IIR-M satellites. Table 3 shows the mean point positioning residuals from L2 and L2C. Both codes were given the same weighting. The mean L2C residuals over all stations were $0{\cdot}87$, $0{\cdot}90$ and $0{\cdot}95$ times the mean L2 residuals for PRNs 12, 15 and 17 respectively. This suggests that the L2C measurements were more precise than L2.

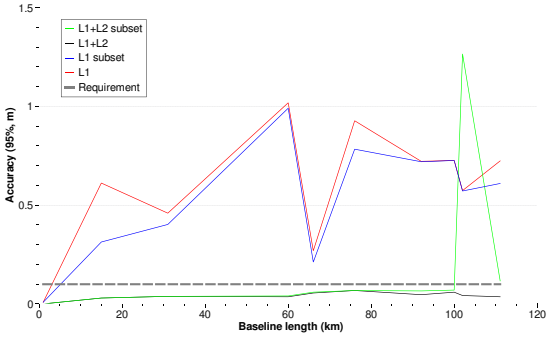

(a) Accuracy

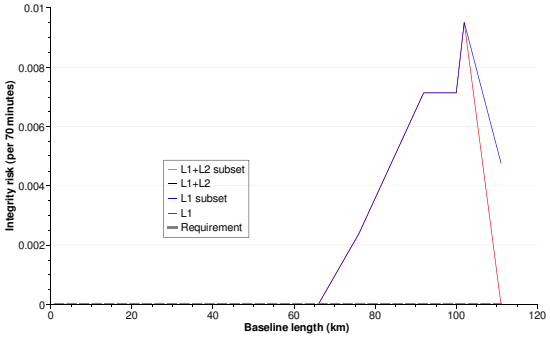

(b) Integrity

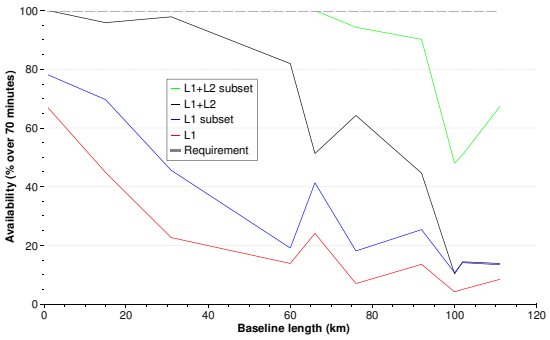

(c) Availability

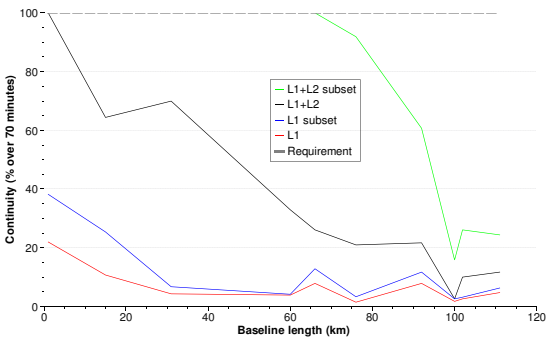

(d) Continuity

Figure 14: RTK results

Table 3: Mean L2 and L2C residuals (m)

	PRN 12		PRN 15		PRN 17	
Station	L2	L2C	L2	L2C	L2	L2C
SHIP	1·880	1·530	1·816	1·499	1·687	1·461
BASE	1·222	0·981	2·107	1·832	2·230	2·076
WIX	1·757	1·441	1·569	1·224	1·791	1·625
MAID	2·926	2·686	2·862	2·806	2·535	2·541
SHOE	2·745	2·518	2·543	2·468	2·377	2·330
STRA	2·722	2·537	2·741	2·687	2·388	2·427

Table 4: Processing techniques matched to requirements, indicating maximum baseline length

Technique	PP	DGPS	RTK	RTK+subset algorithm
Frequencies	L1	L1	L1+L2	L1+L2
Ocean and coastal	Yes	> 110 km	1 km	66 km
Port approach	Yes	> 110 km	1 km	66 km
Port navigation	No	> 110 km	1 km	66 km
Automatic docking	No	No	1 km	66 km

5 Conclusion

Table 4 shows how the different processing techniques are matched to the requirements, giving the maximum achievable baseline length. Accuracy was the limiting factor for PP and DGPS; RTK was limited by the difficulty of achieving correct ambiguity resolution. Single-frequency positioning was as useful as dual-frequency for PP and DGPS for all baseline lengths, but was significantly worse for RTK.

Point positioning is the simplest technique to implement and does not require shore infrastructure, but the accuracy is too low to meet the port navigation or automatic docking requirements. However, the point positioning easily met the requirements for ocean and coastal navigation and port approach. The single-frequency results were almost as good as the dual frequency, and the ionospheric-free combination gave a similar accuracy. Therefore these requirements should be met even in periods of high ionospheric activity.

DGPS is sufficiently accurate to meet the port navigation requirements for long baselines when using both single and dual frequency. However, during a period of high ionospheric activity it might be necessary to use the ionospheric-free observable to eliminate the ionosphere over longer baselines: for this experiment the resultant multiplication of code noise and multipath error would reduce the accuracy to below the port navigation requirements. High ionospheric activity could also reduce the range over which single-frequency DGPS is practicable.

Although RTK is more accurate than either PP or DGPS, the ambiguity resolution step is not very robust, particularly over longer baselines or with single-frequency data. This can result in the ambiguities not being fixed, affecting the continuity and availability, or being fixed incorrectly, causing an integrity error or reducing the accuracy. Because of this, no requirements are met except when using dual-frequency data over the 1 km baseline: in this case the strictest requirements, those for automatic docking, are met.

The subset ambiguity resolution algorithm described in Section 3.5 extends the baseline length over which the automatic docking requirements are met using dual-frequency RTK from to 1 km to 66 km. However, at very long baselines the results were made worse by the propagation of ambiguities that had been fixed incorrectly with LAMBDA. The algorithm is most useful to fill the gaps between successful ambiguity resolution over shorter baselines, where biases that prevent ambiguity resolution, such as multipath, affect different observations differently. Over long baselines, biases such as atmospheric decorrelation affect all observations and therefore provide less scope for successful subset ambiguity resolution. This experiment also demonstrates that it is dangerous to apply this algorithm in situations where the normal ambiguity resolution fixes the ambiguities incorrectly, as these errors are propagated to more epochs.

Due to the small quantity of data analysed, these results do not demonstrate that, in the general case, the IMO requirements can be met as shown in Table 4. However, they do give an indication of which techniques could be used, and which could not, to meet a given set of requirements.

6 Acknowledgements

The authors are grateful to Topcon for supplying manpower and equipment, and Ordnance Survey for supplying reference station data. This work is funded through an EPSRC CASE studentship with the General Lighthouse Authorities of the UK and Ireland.

References

de Halpert J, Basker S, Parkins A (2006) Future trends in shipping and its demand on aids to navigation. In: Aids to Navigation in the Digital World, 16th conference of the International Association of Marine Aids to Navigation and Lighthouse Authorities, Shanghai

IALA (2008) e-Navigation: Frequently asked questions, version 1.1

IMO (2001) Revised maritime policy and requirements for a future global navigation satellite system (GNSS), resolution A.915(22)

IMO (2005) International shipping - carrier of world trade, background Paper, World Maritime Day 2005

IMO (2008) Development of an e-Navigation strategy. COMSAR 12/11

de Jonge P, Tiberius C (1996) The LAMBDA method for Integer Ambiguity Estimation: Implementation Aspects. Delft Geodetic Computing Centre

Kim D, Langley R (2000) GPS ambiguity resolution and validation: Methodologies, trends and issues. In: 7th GNSS Workshop-International Symposium on GPS/GNSS, Seoul, Korea, Nov

Teunissen P (1993) Least-squares estimation of the integer GPS ambiguities. In: Invited Lecture, Section IV Theory and Methodology, IAG General Meeting, Beijing, China, August

Teunissen P (1995) The least-squares ambiguity decorrelation adjustment: a method for fast GPS integer ambiguity estimation. Journal of Geodesy 70(1):65–82

Teunissen P (1999) An optimality property of the integer least-squares estimator. Journal of Geodesy 73(11):587–593

Teunissen P, Odijk D, Jong C (2000) Ambiguity dilution of precision : an additional tool for GPS quality control. In: LGR-Series, 21, Delft Geodetic Computing Centre, Delft, pp 261–270

UNCTAD (2007) Review of maritime transport, 2007, united Nations, New York and Geneva

Verhagen S (2005) The GNSS integer ambiguities: estimation and validation. PhD thesis, Delft University of Technology